# Density functional theory study on the pyrolysis mechanism of thiophene in coal

Li-Xia Ling, Ri-Guang Zhang, Bao-Jun Wang *, Ke-Chang Xie

*Key Laboratory of Coal Science and Technology (Taiyuan University of Technology), Ministry of Education and Shanxi Province, Taiyuan 030024, China*

## ARTICLE INFO

## ABSTRACT

The pyrolysis mechanism of thiophene in coal has been investigated with a density functional theory method. Three intramolecular hydrogen migration reaction paths leading to the formation of $H_2S$ were designed. It can be concluded that the favorable energy path by the kinetic analysis is that the $\alpha$-H migrates to S firstly; then the $\beta$-H migrates to the $\alpha$-C followed by a concerted C–S bond cleavage resulting in the cyclic structure of thiophene turning into a chain structure; finally $H_2S$ and butadiyne are formed via H migrating twice. In the favorable energy path, the rate determining step is the $\alpha$-H migration to S, and the activation energy is about 351.63 kJ mol$^{-1}$ at 298.15 K.

© 2009 Elsevier B.V. All rights reserved.

## 1. Introduction

As one of main energy sources in China, coal has contributed to the development of national economy. But sulfur is a major factor in inhibiting the effective and extensive utilization of coal. Therefore, desulfurization of coal, in order to preserve the environment and eliminate air pollution resulting from the release of sulfur-containing compounds, has long been an important topic [1]. A number of methods have been developed to study the desulfurization, such as biodesulfurization [2], electrochemistry desulfurization [3] and chemistry desulfurization [4]. However, an effective and economic process to remove sulfur has not been found. This is partly due to the fact that the formation mechanism of sulfur-containing compounds during coal pyrolysis is still not perfectly understood.

It is known that the organic sulfur in coal is more complex and is hard to remove [5,6], in which thiophene ($C_4H_4S$) is often used as an organosulfur model to investigate the desulfurization process [7]. Cullis and Norris [8] found that $H_2S$ was formed in large quantities at 1323 K. While Winkler et al. [9] found that the amount of $H_2S$ increased strongly above 1123 K during the continuous flow pyrolysis of thiophene, and fragmental products are also formed from thiophene, such as $C_4H_2$. Memon et al. [10] also detected major gaseous product $H_2S$ when studying pyrolysis of thiophene over the temperature range 1598–2022 K. These all show that $H_2S$ was the major product of thiophene pyrolysis, but no kinetics information was got for the formation of $H_2S$. Recently, a study of the unimolecular decomposition of thiophene was carried out to explain the formation of $H_2S$ [11]. Energies and the bond Mulliken Popula-

tion of several decomposition pathways were analyzed, but no reaction rate constants were calculated and thus no comparison with different paths was made. So it is necessary of a comprehensive quantum chemical study in conjunction with kinetic modeling in order to obtain rate constants for the decomposition reactions and to elucidate the important pathways in the thermal decomposition of thiophene.

So we undertook a density functional theory (DFT) study on the thiophene pyrolysis by searching transition states and possible intermediates of designed three decomposition pathways, and conclude the formation mechanism of $H_2S$ and the migration rule of sulfur in thiophene by analyzing the structure microscopic parameters, thermodynamic function change and kinetic function change, with a view of providing a theoretical reference for desulfurization of coal.

## 2. Computational details

A DFT method was adopted and calculations were performed using the Dmol$^3$ program [12] mounted on Materials studio 4.0 package. All the structures were geometrically optimized at the level of the generalized gradient approximation (GGA) with Perdew–Wang 1991 (PW91) functional [13]. The DND basis set, which is equivalent in accuracy to the 6-31G$^*$ Gaussian orbital basis set, was also used. Spin unrestricted was chosen. Total SCF tolerance criteria, integration accuracy criteria and orbital cutoff quality criteria were set at medium. Multipolar expansion was set at octupole. These parameters and the method are credible to study the thermodynamic properties of sulfur-containing model compounds according to our previous study [14]. The optimized structures were calculated at the same level of theory and vibrational analysis

\* Corresponding author.
*E-mail address:* wangbaojun@tyut.edu.cn (B.-J. Wang).

**Table 1**
Imaginary frequency of each transition state and the bonds corresponding to relative normal vibration.

| Transition state | Imaginary frequency $(cm^{-1})$ | Bond corresponding to normal vibration |
|---|---|---|
| TS1 | −886.96 | C4–H9–S5 |
| TS2 | −209.15 | C3–H8–C4 |
| TS3 | −277.19 | C1–S5–H9 |
| TS4 | −1223.76 | C1–H6–S5 |
| TS5 | −524.84 | C2–H9–C1 |
| TS6 | −992.7 | C1–H6–S5 |
| TS7 | −206.89 | C3–H8–C4 |
| TS5′ | −466.22 | C2–H7–C1 |
| TS8 | −1070.01 | C1–H6–C2 |
| TS9 | −1302.64 | C4–H9–S5 |
| TS10 | −265.71 | C3–H8–C4 |
| TS11 | −118.04 | C2–H6–S5 |
| TS5″ | −581.70 | C2–H7–C1 |

was carried out for each structure to characterize it either as an equilibrium structure (no imaginary frequency) or a transition state (one imaginary frequency whose vibrational mode corresponds to the reaction coordinate), imaginary frequency of each transition state and the bonds corresponding to relative normal vibration in the process of thiophene pyrolysis were shown in Table 1, and TS confirmation calculations were carried out to confirm that the TS leading to the desired reactant and product. Meanwhile, the electronic energy ($E_{elec}$) and Mulliken atomic charges of all structures were calculated, the standard entropy ($S^0$), the enthalpy ($H^0$) and ZPVE were got by frequency analysis. All calculations were performed on HP Proliant DL 380 G5 server system.

## 3. Results and discussion

### 3.1. General reaction paths

Some experiments [10,15] supported that C–S bond fission preceded other reactions and formed biradical during pyrolysis of thiophene. While bond between C and hetero-atom being very strong was concluded by Martoprawiro's investigation on pyrrole decomposition [16], meanwhile, which can also be got from the calculated result (560.00 kJ mol$^{-1}$) [17] of C–S bond strength. Other experiments [18,19] supported that C–H bond was weak, and might cleave initially. So a $\alpha$-H atom abstracted from thiophene was investigated firstly, the calculated bond dissociation energy was about 476.64 kJ mol$^{-1}$, which was in agreement with the C–

H bond strength of 488.18 kJ mol$^{-1}$ [20], but significantly higher than the activation energy of the reaction derived from kinetic data [21]. So the mechanism of $\alpha$-H migration to S as the first step was proposed in Path 1 and Path 2. Besides, Hore's research showed that 1, 2-H migration was the most probable step (activation energy 300.0 kJ mol$^{-1}$) before bond fission of thiophene [17], so Path 3 was proposed. The possible reaction mechanism of thiophene pyrolysis was shown in Fig. 1.

### 3.2. Path 1 and Path 2: the formation process of $H_2S$ via $\alpha$-H migration to S as the first step

The optimized structures and their atom numbers of reactants, intermediates, transition states and products in Path 1 and Path 2 are shown in Fig. 2, and the relevant energies of the stationary points for the two paths are shown in Fig. 3. Initially, $\alpha$-H9 migrates from C4 to S5 followed by C4–H9 bond cleavage and S5–H9 bond formation via TS1 with only one imaginary frequency. The energy barrier of 351.63 kJ mol$^{-1}$ is needed in this H migration process, which is smaller than that of C–H bond fission. The heavy atom skeleton of the transition state, TS1, is nearly planar while the migrating hydrogen is out of plane of the heavy atom skeleton. The intermediate, IM1, has $C_1$ symmetry and possesses a biradical nature with $\sigma$-type electronic distribution. In this step, The $C_{2v}$ symmetry of thiophene is destroyed along with the H migration, and the Mulliken atomic charges of C1 and C4 become different, are −0.207 and −0.159 (see from Table 2), respectively. The $\pi$-6 conjugate system of thiophene is also destroyed. Then H8 in IM1 migrates from C3 to C4 followed by C4–S5 cleavage, and the bond length alternates from 1.808 to 3.930 Å, which shows that the cyclic structure of thiophene turns into a chain structure. C3–C4 bond has a property of triple bond due to this bond shortening from 1.378 to 1.217 Å, and the angle of $\angle$C2–C3–C4 and $\angle$C3–C4–H8 are close to 180°. The Mulliken atomic charge of C4 becomes more negative, which can be explained that the $sp^2$ hybridization of C3 and C4 in IM1 is turned into $sp$ hybridization of them in IM2, and the formation of triple bond of C3–C4 leads to the acidity of H8. In this step, TS2 is 85.39 kJ mol$^{-1}$ higher in energy than IM1. The *trans* structure IM2 isomerizes to *cis* isomer IM3 in Step3 (IM2 → IM3), it can be seen that H9 deflects by $\angle$C4–S5–H9 changing from 159.323° to 30.889°, this isomerization process with an energy barrier of 28.55 kJ mol$^{-1}$ via TS3. Step4 (IM3 → IM4) is also a H migration process, the bond lengths and angles have little change except the bond linking with H6, and a high energy barrier of 348.36 kJ mol$^{-1}$ is needed because the intermediate IM3 is sta-
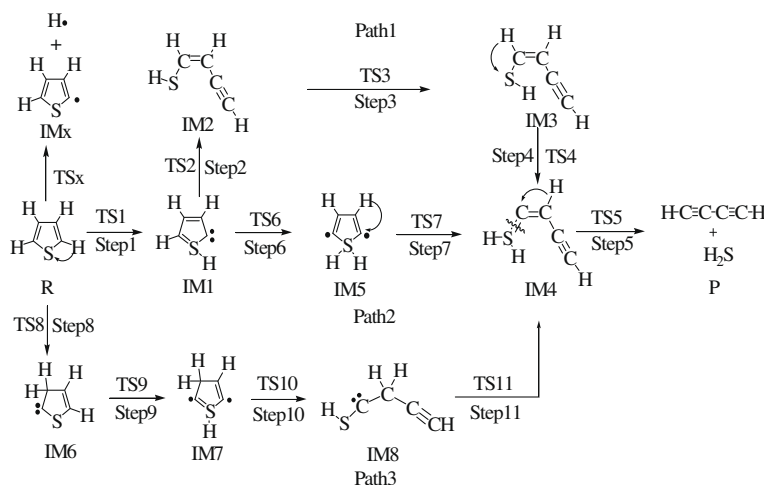


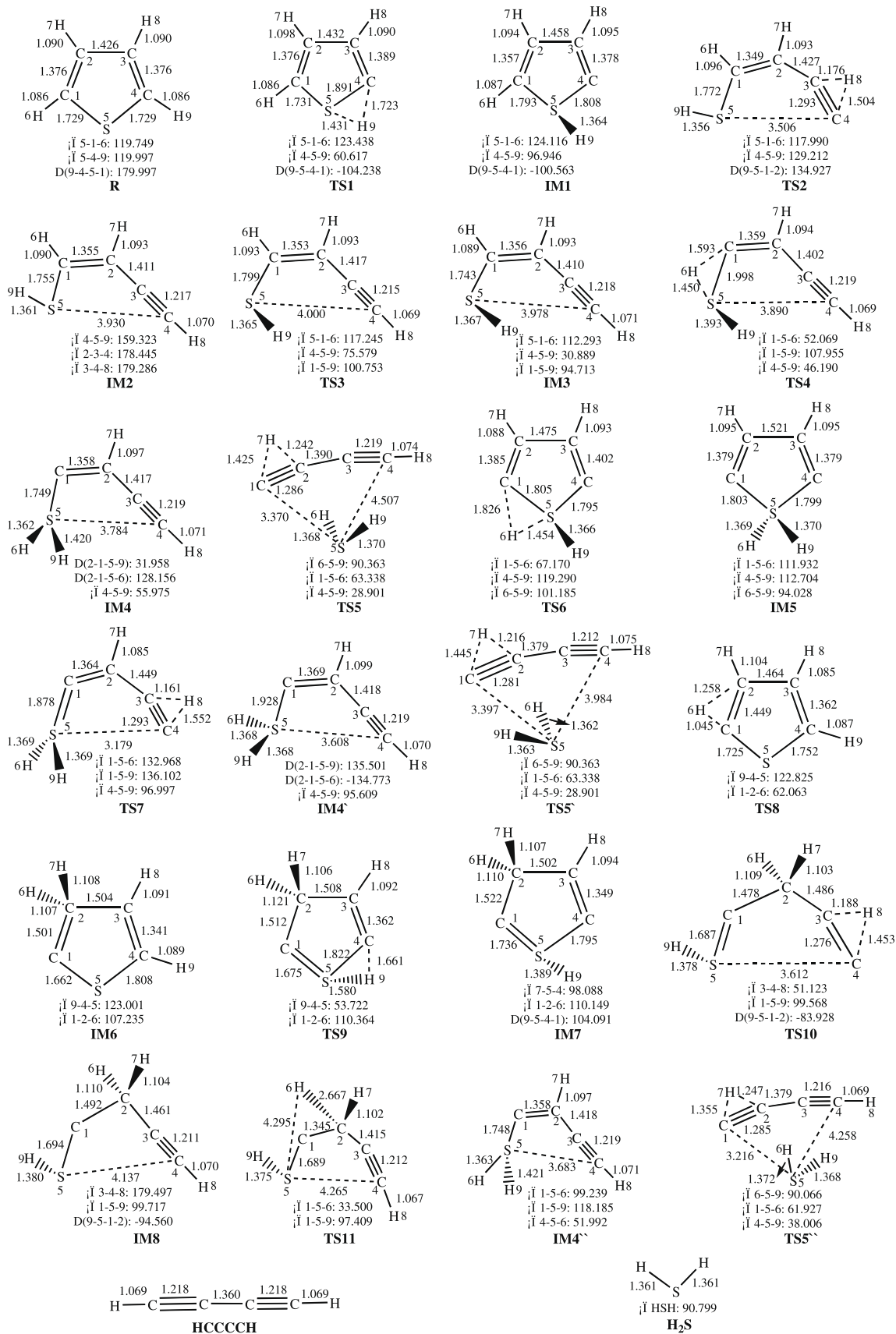**Fig. 1.** The proposed reaction mechanism of thiophene pyrolysis.

**Fig. 2.** The optimized geometries of all reactant, intermediates, transition states and products in three reaction paths.
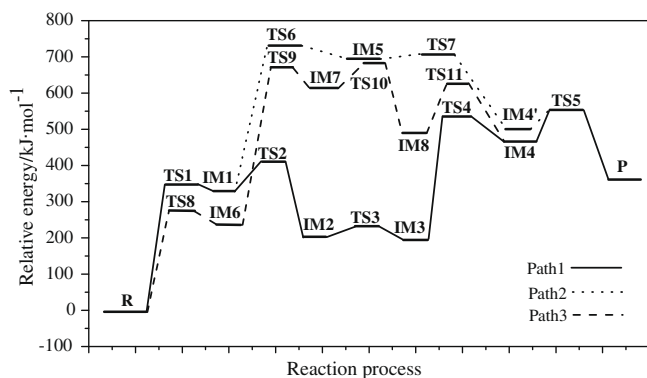
**Fig. 3.** Energies sketch of the stationary points for the three paths.

bler than other intermediates. The last step (Step5) in Path 1, H7 migrates from C2 to C1, the $H_2S$ separates from the original structure and butadiyne is formed, which is a concerted process.

In Path 2, H6 in IM1 migrates from C1 to S5 leading to the formation of IM5, which has $C_{2v}$ symmetry and two unpaired electrons, a $\sigma$-electron locates in the C4 and the other $\sigma$-electron locates in the C1. The energy barrier of 403.72 kJ mol$^{-1}$ is needed in this step, which is higher than that of Step1. Then H8 migrates from C3 to C4, the cyclic structure of thiophene has been destroyed and a chain structure is formed as the bond length of C4–S5 alternates from 1.799 to 3.608 Å, leading to the formation of IM4′. IM4′ has similar structure with IM4, but they have different dihedral angles of C2–C1–S5–H9 and C2–C1–S5–H6, and the energy of IM4′ is 33.00 kJ mol$^{-1}$ higher than that of IM4. At last, H7 migration from C2 to C1 leads to the deprivation of $H_2S$ via TS5′, which has almost the same energy with TS5, and the structures have little differences.

### 3.3. Path 3: the formation process of $H_2S$ via 1,2-H migration as the first step

1,2-H migration as the first step was also designed to investigate the formation of $H_2S$. The relevant energies of the stationary points for Path 3 are also shown in Fig. 3. In Step8, $\alpha$′-H6 migrates from C1 to C2 via TS8 with an imaginary frequency of −1070.01 cm$^{-1}$, a lower energy barrier of 279.29 kJ mol$^{-1}$ than Step1 is needed, which leads to the formation of IM6. IM6 has a carbonic characteristic and a lone pair of unpaired electrons with $\sigma$-type locates in C1 atom. Then $\alpha$-H9 migrates from C4 to S5 with a higher energy barrier of 432.35 kJ mol$^{-1}$, and forming IM7, which has an unpaired $\sigma$-electron locating in the C4 and the other $\sigma$-electron locating in the C1. And followed by H8 migrating from C3 to C4, the cyclic structure is turned into a chain structure leading to the formation of IM8, an energy of 76.68 kJ mol$^{-1}$ is needed. IM8 has a carbonic characteristic and a lone pair of unpaired electrons with $\sigma$-type locates in C1 atom. From IM8, H6 migrates from C2 to S5 to form IM4″. IM4″ has similar structure and energy with IM4, the difference can be seen in Fig. 2. Then H7 migrates from C2 to C1 leading to the formation of $H_2S$, which is similar to the Step5.

### 3.4. The kinetic analysis of all paths

The detailed kinetic analysis of three pathways will be discussed in this section. According to the transition state theory, activation enthalpy $\Delta_r H^{\neq}_m$, activation entropy $\Delta_r S^{\neq}_m$ and activation energy $E_a$ can be got from Eqs. (1)–(3), respectively. The rate constant $k$ can be expressed in Eq. (4).

$$\Delta_r H^{\neq}_m = H(TS) - H(R) \tag{1}$$

$$\Delta_r S^{\neq}_m = S(TS) - S(R) \tag{2}$$

$$E_a = \Delta_r H^{\neq}_m + nRT \tag{3}$$

$$k = \frac{k_b T}{h} \left(\frac{p^o}{RT}\right)^{1-n} \exp\left(\frac{-E_a}{RT}\right) ([22]) \tag{4}$$

where $k$ is the rate constant, $T$ is reaction temperature, $k_b$, $h$, $p^0$ and $R$ are Boltzman constant, Blank constant, standard atmospheric pressure and fundamental gas constant, $n$ is the number of reactant.

Table 3 gives $\Delta_r H^{\neq}_m$, $\Delta_r S^{\neq}_m$, $E_a$ and the rate constant $\ln k$ of every elementary reaction at the temperature 298.15 and 875 K. In Path 1, it can be seen that the activation energy of Step3 (IM2 → IM3) is the smallest, and the rate constant $\ln k_3$(298.15 K) is higher than others. It shows that Step3 occurs easily. Meanwhile, from the molecular structures of transition state and the reactant, we can see that this step is a *cis–trans* isomerization process, and no bond cleavage nor new bond formation, which facilitates the reaction of Step4. The activation energy of Step1 (R → IM1) is the highest, and the rate constant $\ln k_1$ is the smallest, so it can be concluded that Step1 is the rate determining step in Path 1. It is an H migration process, and the aromaticity of thiophene destroyed. The increase in reaction temperature is in favor of the pyrolysis reaction of thiophene under isothermal and isotonic conditions by comparing to the rate constants at different temperatures.

In Path 2, from the activation energy and rate constant, we can see that the activation energy of Step6 is the highest, and the rate constant $\ln k_6$ is the smallest, so it can be concluded that the Step6 is the rate determining step in Path 2. In Path 3, the activation energy of Step9 is the highest.

Comparing with the three paths, it is concluded that the activation energy of rate determining step (Step1) of Path 1 is 52.09 kJ mol$^{-1}$ smaller than that of Step6 in Path 2, and is 80.72 kJ mol$^{-1}$ smaller than that of Step9 in Path 3, $\ln k_6$ and $\ln k_9$ are both smaller than $\ln k_1$, so we conclude that Path 1 is the favorable energy path.

## 4. Conclusions

The calculated structure microscopic parameters, thermodynamic and kinetic changes of the pyrolysis pathways of thiophene show that:

1. All transition states and intermediates in the three reaction paths of thiophene pyrolysis were determined.
2. The favorable energy path in three paths is that the $\alpha$-H migrates to S firstly, which is the rate determining step; then the $\beta$-H migrates to the $\alpha$-C followed by a coordianted C–S bond

**Table 2**
Mulliken atomic charges analysis of all structures in Path 1.

|       | R      | TS1    | IM1    | TS2    | IM2    | TS3    | IM3    | TS4    | IM4    | TS5    | P      |
|-------|--------|--------|--------|--------|--------|--------|--------|--------|--------|--------|--------|
| C(1)  | −0.149 | −0.174 | −0.207 | −0.128 | −0.105 | −0.137 | −0.077 | −0.209 | −0.094 | −0.252 | −0.349 |
| C(2)  | −0.150 | −0.101 | −0.103 | −0.187 | −0.264 | −0.211 | −0.266 | −0.295 | −0.296 | −0.078 | 0.154  |
| C(3)  | −0.151 | −0.202 | −0.215 | −0.067 | 0.170  | 0.184  | 0.173  | 0.195  | 0.178  | 0.171  | 0.155  |
| C(4)  | −0.149 | −0.186 | −0.159 | −0.188 | −0.340 | −0.316 | −0.344 | −0.346 | −0.359 | −0.309 | −0.352 |
| S(5)  | −0.103 | −0.158 | −0.133 | −0.290 | −0.271 | −0.339 | −0.316 | −0.292 | −0.255 | −0.459 | −0.499 |

**Table 3**
The activation energy and rate constant of elementary reaction.

| Elementary reaction | $\Delta_r H_m^{\neq}$ (kJ mol$^{-1}$) | | $\Delta_r S_m^{\neq}$ (J mol$^{-1}$ K$^{-1}$) | | $E_a$ (kJ mol$^{-1}$) | | ln$k$ (s$^{-1}$) | |
|---|---|---|---|---|---|---|---|---|
| | 298.15 K | 875 K | 298.15 K | 875 K | 298.15 K | 875 K | 298.15 K | 875 K |
| *Path 1* | | | | | | | | |
| Step1 | 349.15 | 348.67 | 4.30 | 3.97 | 351.63 | 355.95 | −112.40 | −18.40 |
| Step2 | 82.91 | 81.88 | 27.92 | 27.29 | 85.39 | 89.15 | −4.99 | 18.28 |
| Step3 | 26.07 | 21.11 | −13.37 | −22.64 | 28.55 | 28.39 | 17.94 | 26.63 |
| Step4 | 345.88 | 347.14 | 18.63 | 21.83 | 348.36 | 354.42 | −111.08 | −18.18 |
| Step5 | 94.06 | 95.54 | 43.39 | 47.82 | 96.54 | 102.82 | −9.49 | 16.40 |
| *Path 2* | | | | | | | | |
| Step1 | 349.15 | 348.67 | 4.30 | 3.97 | 351.63 | 355.95 | −112.40 | −18.40 |
| Step6 | 401.24 | 400.37 | 9.42 | 8.22 | 403.72 | 407.64 | −133.41 | −25.50 |
| Step7 | 5.10 | 4.12 | 23.98 | 23.38 | 7.58 | 11.40 | 26.40 | 28.97 |
| Step5′ | 60.89 | 62.00 | 35.08 | 38.69 | 63.37 | 69.26 | 3.89 | 21.01 |
| *Path 3* | | | | | | | | |
| Step8 | 276.82 | 274.88 | −0.30 | −3.68 | 279.29 | 282.15 | −83.22 | −8.25 |
| Step9 | 429.87 | 430.88 | 2.83 | 5.16 | 432.35 | 438.16 | −144.96 | −29.70 |
| Step10 | 74.20 | 73.90 | 48.35 | 49.29 | 76.68 | 81.17 | −1.47 | 19.38 |
| Step11 | 136.38 | 139.92 | 22.98 | 30.61 | 138.86 | 147.20 | −26.56 | 10.30 |
| Step5″ | 97.04 | 99.30 | 43.23 | 49.42 | 99.52 | 106.58 | −10.69 | 15.88 |

cleavage resulting in the cyclic structure of thiophene changing into a chain structure; finally $H_2S$ and butadiyne are formed via H migration twice.

3. Intramolecular H migration exists universally and plays an important role in thiophene pyrolysis.
4. The thiophene pyrolysis is an endothermal reaction, and increasing temperature is in favor of the pyrolysis of thiophene.

## References

[1] H.K. Chen, B.Q. Li, J.L. Yang, B.J. Zhang, Fuel 77 (1998) 487.
[2] J. Klein, Biodegradation 9 (1998) 293.
[3] Z.C. Wang, W.R. Yao, P. Cui, T. Song, J. Fuel Chem. Tech. 31 (2003) 509.
[4] Z.Q. Gao, X.D. Hu, Y.Q. Wu, J.S. Gao, Environ. Chem. 13 (1994) 486.
[5] L. Xu, J.L. Yang, Y.M. Li, Z.Y. Liu, Fuel Process. Technol. 85 (2004) 1013.
[6] P. Selsbo, P. Almén, I. Ericsson, Energy Fuel 10 (1996) 751.
[7] P. Mills, S. Korlann, M.E. Bussell, M.A. Reynolds, M.V. Ovchinnikov, R.J. Angelici, C. Stinner, T. Weber, R. Prins, J. Phys. Chem. A 105 (2001) 4418.
[8] C.F. Cullis, A.C. Norris, Carbon 10 (1972) 525.
[9] J.K. Winkler, W. Karow, P. Rademcher, J. Anal. Appl. Pyrol. 62 (2002) 123.
[10] H.U.R. Memon, A. Williams, P.T. Williams, Int. J. Energy Res. 27 (2003) 225.
[11] C. Huang, J.Y. Zhang, J. Chen, C.G. Zheng, Coal Conversion 28 (2005) 33.
[12] B. Delley, J. Chem. Phys. 113 (2000) 7756.
[13] J.P. Perdew, J.A. Chevary, S.H. Vosko, K.A. Jackson, M.P. Pederson, D.J. Singh, C. Fiolhais, Phys. Rev. B 46 (1992) 6671.
[14] L.X. Ling, L.J. Zhao, B.J. Wang, in: Proceedings of the ninth China–Japan Symposium on Coal and C1 Chemistry, Chengdu, China, 22–28 October, 2006.
[15] M. Bajus, V. Veselý, J. Baxa, Ind. Eng. Chem. Prod. Res. Dev. 20 (1981) 741.
[16] M. Martoprawiro, G.B. Bacskay, J.C. Mackie, J. Phys. Chem. A 103 (1999) 3923.
[17] N.R. Hore, D.K. Russell, New J. Chem. 28 (2004) 606.
[18] C.D. Hurd, R.V. Levetan, A.R. Macon, J. Am. Chem. Soc. 84 (1962) 4515.
[19] O.S.L. Bruinsma, P.J.J. Tromp, H.J.J. De Sauvage Nolting, J.A. Moulijn, Fuel 67 (1988) 334.
[20] C. Barckholtz, T.A. Barckholtz, C.M. Hadad, J. Am. Chem. Soc. 121 (1999) 491.
[21] J.C. Mackie, M.B. Colket, P.F. Nelson, M. Esler, Int. J. Chem. Kinet. 23 (1991) 733.
[22] B.J. Wang, X.Y. Wei, K.C. Xie, Chin. J. Chem. Eng. 55 (2004) 569.